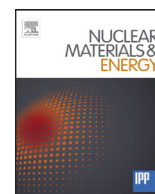


Contents lists available at [ScienceDirect](http://ScienceDirect)

## Nuclear Materials and Energy

journal homepage: [www.elsevier.com/locate/nme](http://www.elsevier.com/locate/nme)

## Surface cracking of tungsten-vanadium alloys under transient heat loads

Kameel Arshad<sup>a</sup>, Dan Ding<sup>a</sup>, Jun Wang<sup>a</sup>, Yue Yuan<sup>a,\*</sup>, Zheng Wang<sup>a</sup>, Ying Zhang<sup>a</sup>,  
Zhang-jian Zhou<sup>b</sup>, Xiang Liu<sup>c</sup>, Guang-Hong Lu<sup>a,\*</sup><sup>a</sup> School of Physics and Nuclear Energy Engineering, Beihang University, Beijing 100191, China<sup>b</sup> School of Materials Science and Engineering, University of Science and Technology Beijing (USTB), Beijing 100083, China<sup>c</sup> Southwestern Institute of Physics, P.O. Box 432, Chengdu 610041, Sichuan, China

## ARTICLE INFO

## Article history:

Received 22 April 2015

Revised 17 May 2015

Accepted 18 May 2015

Available online 28 August 2015

## Keywords:

W-V alloys

Plasma facing materials

Transient heat loads

Surface cracking

## ABSTRACT

To evaluate high heat load performance of tungsten-vanadium (W-V) alloys as a potential candidate for plasma facing materials of fusion devices, the target materials with three different V concentrations (1, 5 and 10 wt%) are exposed to thermal shock loading. The alloys are fabricated by cold isostatic pressing and subsequently sintered in a vacuum furnace. Thereafter, they are exposed to different high heat flux densities ranging from 340 to 675 MW/m<sup>2</sup> for single shot of 5 ms duration in an intense electron beam test facility. The alloys with lowest V concentration (1 wt%) are highly damaged in form of seriously cracking. The ones with intermediate V content (5 wt%) has shown comparatively better performance than both highest and lowest V contents alloys. The results indicate that improved mechanical properties and reduced thermal conductivity due to V addition comprehensively affect the cracking behavior of W-V alloy under transient thermal shock.

© 2015 The Authors. Published by Elsevier Ltd.

This is an open access article under the CC BY-NC-ND license (<http://creativecommons.org/licenses/by-nc-nd/4.0/>).

## 1. Introduction

In the experimental fusion reactor ITER, the first wall materials will face steady-state high heat loads of  $\sim 1$  MW/m<sup>2</sup>, however it is about 10–20 times higher for critical components such as limiter and divertor [1]. Besides, the divertor armor should also bear several types of transient thermal pulses, such as plasma disruptions, vertical displacement events (VDEs) and edge localized modes (ELMs) [2]. These transient loads deposit high energy density of several MJ/m<sup>2</sup> onto the surface of plasma facing materials (PFMs) [3]. As a consequence, thermal loads induced crack formation, melting, melt layer ejection and particle emission will significantly reduce the lifetime of PFMs [4]. Thus the heat high flux (HHF) testing of PFMs is a very important issue in fusion research.

Tungsten (W) and W-based materials due to their excellent physical properties at evaluated temperatures are candidates for PFMs in controlled thermonuclear fusion devices [5–7]. Tungsten-vanadium (W-V) alloys developed for plasma facing application have shown good capability toward improvement in mechanical properties and thermal stability of the microstructures as compared to W [8–10]. However, the testing of these newly developed materials under transient heat loads has not been reported yet. In this study, we

investigate the performance, especially surface cracking, of different grades of W-V alloys under single pulse thermal shock loads.

## 2. Materials

The target materials are fabricated by powder metallurgy process from W and V powders with particle size of 2 and 0.8  $\mu$ m, respectively. W powder is purchased from Beijing Xing Rong Yuan Technology Co., Ltd, and V powder from Shanghai St-Nano Science & Technology Co., Ltd. The powders are mechanically alloyed in a molybdenum high energy ball miller with ball to powder ratio of 5:1 in a speed of 300 rpm for 30 h. The mechanical alloyed powders of three different V concentrations 1, 5 and 10 wt%, identified as W-1 V, W-5 V and W-10 V, respectively, are then compacted by cold isostatic pressing and subsequently consolidated in a vacuum furnace at 2073 K for 2 h. The sintered samples are obtained in the form of rods with 10 cm in length and 12 mm in diameter. Finally, they are cut into 2 mm-thick discs and mechanically polished for HHF experiments. The summary of densities and Vickers micro-hardness of developed specimens is tabulated in Table 1.

As these materials are sintered materials without any post process, in the first step of research and development, their measured relative density is well below 100%. However, post-processing like hot rolling can improve the density near to 100% and can enhance its related properties.

\* Corresponding authors.

E-mail addresses: [yueyuan@buaa.edu.cn](mailto:yueyuan@buaa.edu.cn) (Y. Yuan), [lgh@buaa.edu.cn](mailto:lgh@buaa.edu.cn) (G.-H. Lu).

**Table 1**  
Density and micro-hardness measurements of as sintered W and W-V alloys.

| Samples | V concentration (wt%) | Relative density (%) | Micro-hardness (HV) |
|---------|-----------------------|----------------------|---------------------|
| W-1V    | 1                     | 90.8                 | 428.6               |
| W-5V    | 5                     | 92.23                | 562.3               |
| W-10V   | 10                    | 93.7                 | 686.4               |

### 3. Transient heat load tests

The transient heat load experiments are performed at the Electron-beam Material-test Scenario 60 kW (EMS-60) facility. EMS-60 is capable to produce an energetic electron beam with a maximum accelerating voltage of 150 kV and an intense electron current density. It can work in both single shot and repetitive pulse mode. The samples are mounted on a copper holder with efficient cooling system to keep the base temperature at room temperature. The heat loading tests are performed with single shot pulse of 5 ms and with an accelerating voltage of 120 kV. Loading focuses on a small area of  $4 \times 4 \text{ mm}^2$  on the target surface. The absorbed heat power density can be calculated from the following Eq. (1).

$$P_{abs} = U \times J \times A \quad (1)$$

where  $P_{abs}$ ,  $U$ ,  $J$  and  $A$  are absorbed heat power density ( $\text{MW/m}^2$ ), accelerating voltage (kV), applied beam current density ( $\text{mA/mm}^2$ ) and absorption coefficient for electrons, respectively. The absorption coefficient ( $A$ ) is measured from the ratio of the peak current through the target samples (as shown in Fig. 1) to the applied beam current. The electron absorption coefficient for W-1 V, W-5 V and W-10 V are measured as 0.46, 0.47 and 0.48, respectively. A slight fluctuation in the current profile of electron beam can be seen in Fig. 1 and this nano time scale oscillation pattern was approximately similar for all applied HHF densities. However, the average maximum height of the pulse has been selected for heat power density calculations. Further, such nano time scale fluctuation are normal for such experiments performed by electron beam facilities [11] and do not drastically affect the experimental results.

The temperature of loaded surface is monitored by two optical pyrometers which are calibrated by thermocouple before the HHF testing. Fig. 2 shows transient heat flux dependence of peak temperatures for different grades of W-V alloys. It can be seen clearly that the peak temperature increases monotonically with increasing HHF density. Under similar loading conditions, the surface temperature of W-1 V is always the lowest, where W-10 V is the highest. All the peak surface temperatures are well below melting point of the tested targets. The surface temperature strongly depends on the thermal conductivity of targets. It is worth to note that the thermal conductivity of V is much lower than W, the thermal conductivity of V is  $30.7 \text{ W m}^{-1} \text{ K}^{-1}$  and W is  $173 \text{ W m}^{-1} \text{ K}^{-1}$  at room temperature and V is  $\sim 42.1 \text{ W m}^{-1} \text{ K}^{-1}$  and W is  $\sim 116 \text{ W m}^{-1} \text{ K}^{-1}$ , at 1300 K, respectively. Therefore, the increase of V concentration obviously decreases the thermal conductivity of W-V alloys, and results in the large difference in the surface temperatures for different grades W-V alloys under similar heat loading.

### 4. Surface cracking

The surface modification of the loaded W-V alloys is analyzed by scanning electron microscopy (SEM) and the key crack parameters, such as the crack width, crack distance (distance between adjacent cracks) and density of the crack networks, are extracted from SEM images. An overview of the average (avg.) values of crack width, crack distance and density of the crack networks for all cracked surfaces of W-V alloys tested under different transient loads are summarized in Table 2.

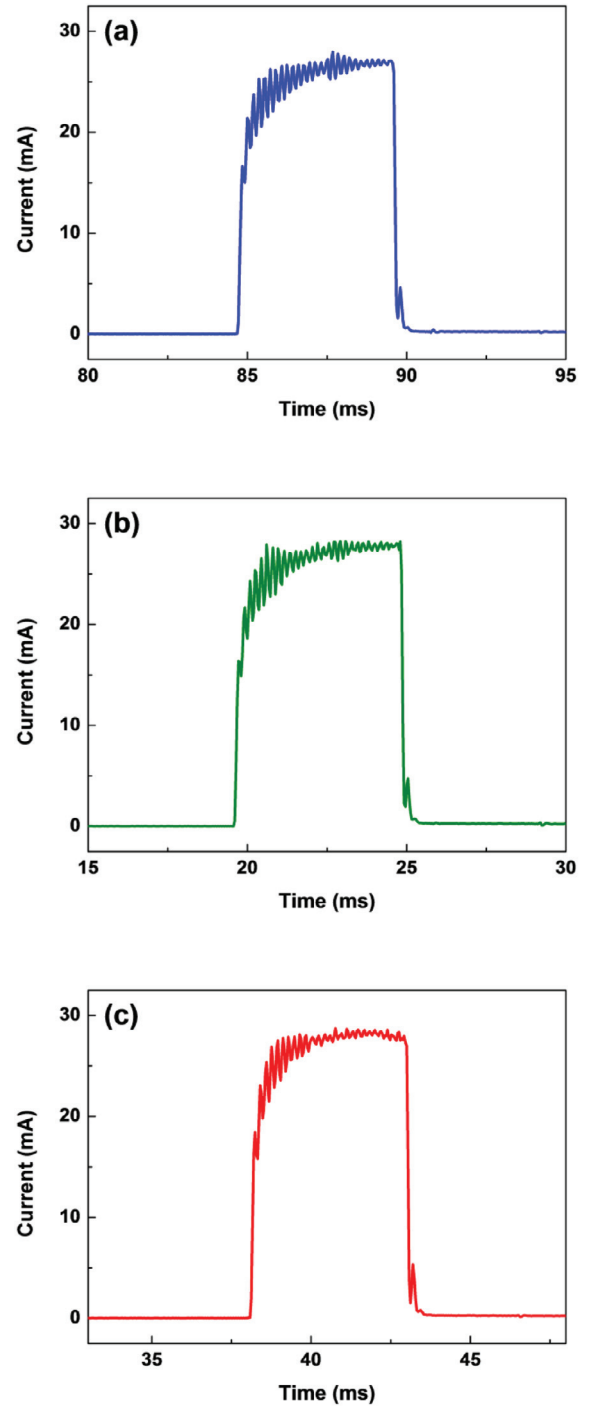


**Fig. 1.** Through-current profiles of the developed materials under 60 mA applied pulse (a) W-1 V, (b) W-5 V and (c) W-10 V, respectively.

Fig. 3(a) shows the surface morphologies of W-1 V after the single pulse heat loading of  $155 \text{ MW/m}^2$ . Obvious cracks are observed with an average width of  $0.6 \mu\text{m}$ , average distance of  $90.9 \mu\text{m}$  and number density of  $127 \text{ cracks/mm}^2$ , respectively. Fig. 3(b) shows that as the HHF density is raised to  $207 \text{ MW/m}^2$ , the average crack width is increased to  $1.0 \mu\text{m}$ , while almost no change in the average crack distance ( $89.3 \mu\text{m}$ ) and crack density ( $131 \text{ cracks/mm}^2$ ) is observed. When the HHF density further increases to  $311 \text{ MW/m}^2$ , W-1 V target is highly degraded as shown in Fig. 3(c). Although the cracking network with a crack density of  $110 \text{ cracks/mm}^2$  is relatively reduced, a prominent increase in the average crack width and crack distance of

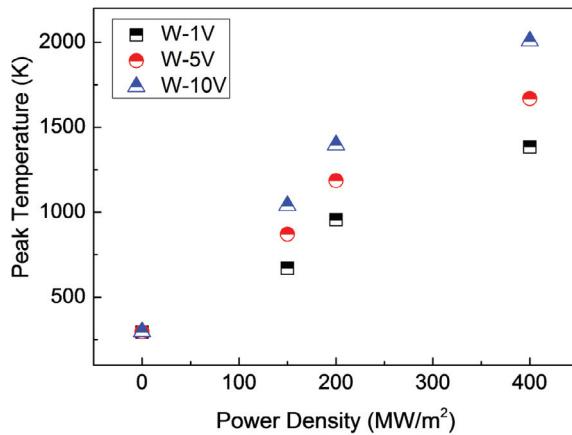


**Fig. 2.** Peak surface temperatures of W-V alloys under 5 ms single shot pulse with different HHF density.

**Table 2**

Average values for crack width, length and number density on the surface of W-V alloys exposed to high transient loads.

| Samples | Power density (MW/m <sup>2</sup> ) | Avg. crack width (μm) | Avg. distance (μm) | Crack number density (cracks/mm <sup>2</sup> ) |
|---------|------------------------------------|-----------------------|--------------------|--|
| W-1V    | 155                                | 0.6                   | 90.9               | 127  |
|         | 207                                | 1.0                   | 89.3               | 131  |
|         | 311                                | 2.7                   | 101.5              | 110  |
| W-5V    | 159                                | No cracks             | No cracks          | No cracks                                      |
|         | 212                                | 1.3                   | 571.4              | 18   |
|         | 317                                | 2.9                   | 589.2              | 8  |
| W-10V   | 162                                | No cracks             | No cracks          | No cracks                                      |
|         | 216                                | 1.0                   | 112.7              | 59   |
|         | 324                                | 2.5                   | 197.1              | 23   |

2.7 and 101.5 μm, respectively is measured for this heavily damaged W-1 V sample.

The surface morphologies and cracking behavior of W-5 V irradiated at different HHF densities are shown in Fig. 4. No cracks are observed on its surfaces tested at 159 MW/m<sup>2</sup> as shown in Fig. 4(a). When the HHF density increases to 212 MW/m<sup>2</sup> (Fig. 4(b)), the W-5 V sample cracks with the crack number density and crack width of 18 cracks/mm<sup>2</sup> and 1.3 μm, respectively. As the HHF density is further increased to 317 MW/m<sup>2</sup> (Fig. 4(c)), the number density of the crack networks is relatively reduced to 8 cracks/mm<sup>2</sup>, but the crack width significantly increases to 2.9 μm, reflecting the worse damage due to increasing HHF density. Compared to W-1 V, one can see that W-5 V shows a better stability against transient thermal shock.

Fig. 5 shows the crack pattern on the loaded surface of W-10 V targets. No cracks are observed on the surface exposed to 162 MW/m<sup>2</sup> as shown in Fig. 5(a). When the HHF density increases to 216 MW/m<sup>2</sup> some cracks appear as shown in Fig. 5(b). The average crack width and distance is about 1.0 and 112.7 μm, respectively. The crack number density of W-10 V (59 cracks/mm<sup>2</sup>) is about two times higher than W-5 V (18 cracks/mm<sup>2</sup>). However, the surface morphology and crack parameters of W-10 V are better than W-1 V under the similar heat loading. Fig. 5(c) shows the surface damage of W-10 V after HHF loading of 324 MW/m<sup>2</sup>. An increase in the crack width is observed, though the crack number density is dropped. Again the surface damage of W-10V at the highest tested HHF density is more severe than W-5 V. Hence, the sintered W-V alloy with intermediate V concentration (5 wt%) has shown relatively better performance at all applied HHF densities than both W-1 V and W-10 V in the present work.

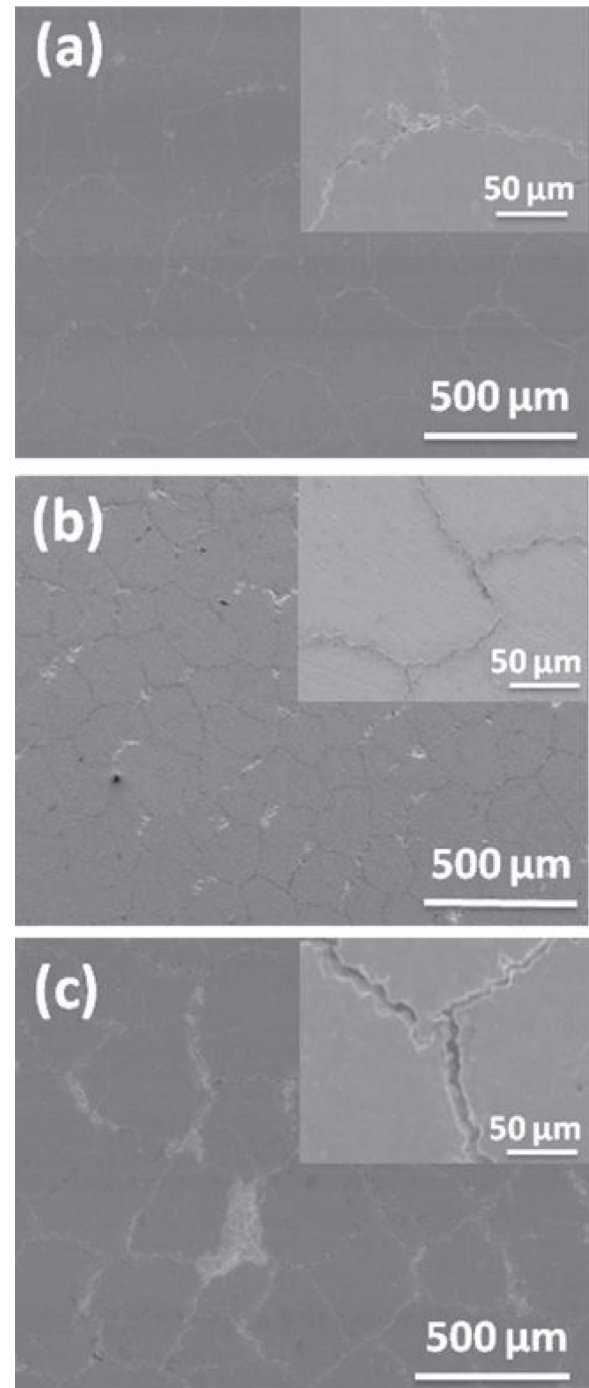


**Fig. 3.** SEM images of the loaded W-1 V surfaces under different HHF density (a) 155 MW/m<sup>2</sup>, (b) 207 MW/m<sup>2</sup> and (c) 311 MW/m<sup>2</sup>.

## 5. Discussion

Different grades of W-V alloys prepared by the same metallurgical route are comparatively tested under transient heat loads. To ensure intense crack networks, all targets are exposed to dense electron beam at room temperature below the ductile-brittle transition temperature (DBTT) [12]. Previously, the addition of V in W has proven to provide great improvement in various properties such as refining the W-matrix microstructure and improving the densification and mechanical properties [9]. Fine-grained microstructure for W materials is important in terms of reduction in brittleness and improvement

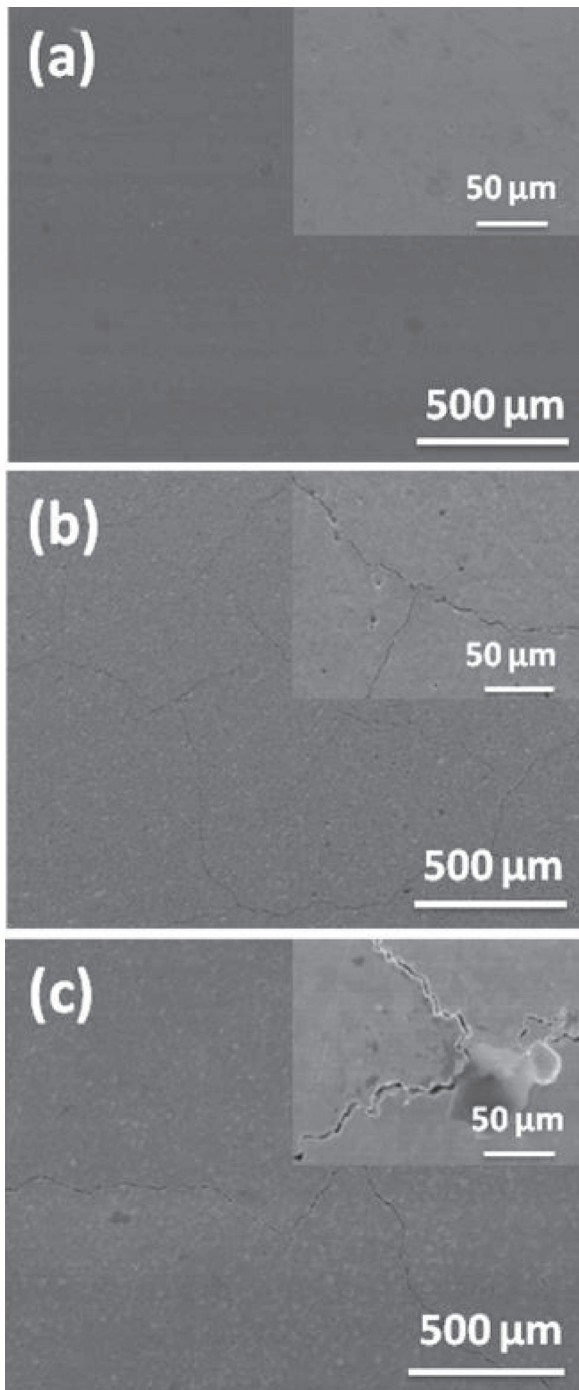


**Fig. 4.** SEM images of the loaded W-5 V surfaces under different HHF density (a) 159 MW/m<sup>2</sup>, (b) 212 MW/m<sup>2</sup> and (c) 317 MW/m<sup>2</sup>.

in toughness and strength [13,14]. The fracture toughness of the W-V alloys gradually improves with the increase of V contents [9]. The mechanical properties of W-based materials at higher temperatures (especially higher than the recrystallization temperature) are highly degraded [13,14]. V addition also enhances the thermal stability of the microstructures and mechanical properties of W-based materials during conventional heating process [10]. However, to assess the newly developed alloys for plasma facing applications, it needs an exposure to fusion relevant conditions. Transient heat loads are the most damaging and important factor for PFMs in fusion reactors research.

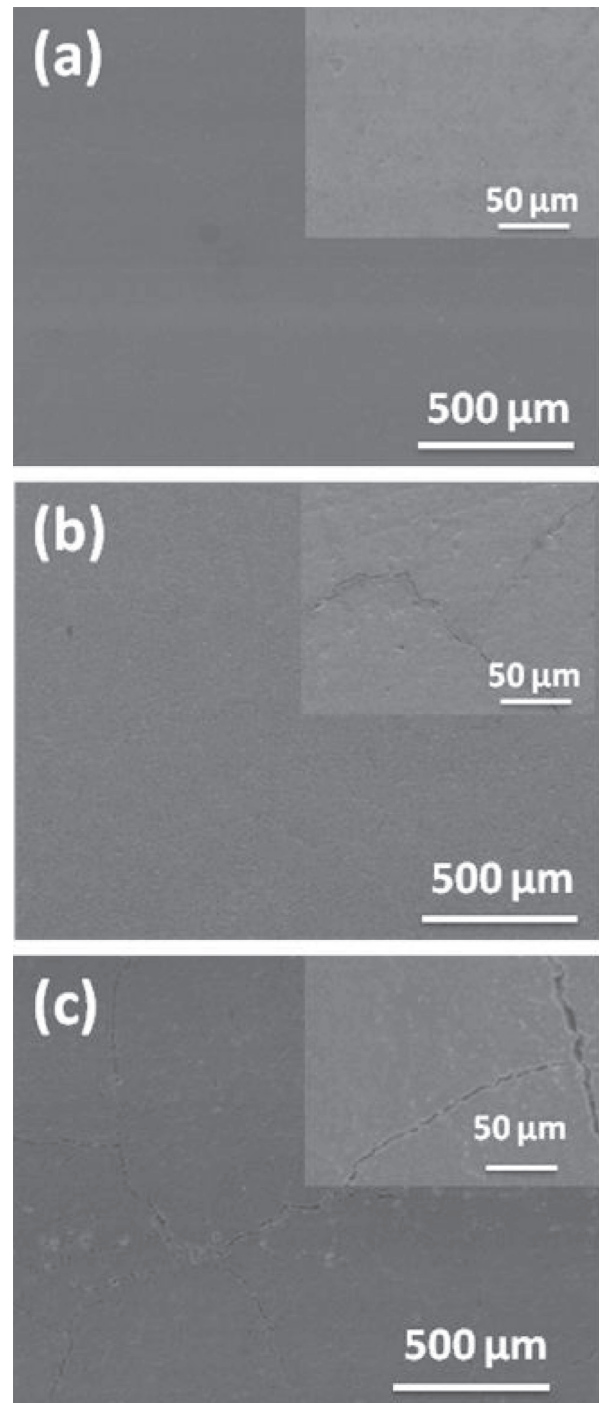


**Fig. 5.** SEM images of the loaded W-10 V surfaces under different HHF density (a) 162 MW/m<sup>2</sup>, (b) 216 MW/m<sup>2</sup> and (c) 324 MW/m<sup>2</sup>.

Comparatively, W-1 V shows the lowest cracking threshold, and comparative higher threshold is similar for the other two alloys. In addition, the cracking width is almost the same for both W-5 V and W-10 V, but W-5 V has lower crack number density. This implies that W-10 V has relatively lower cracking resistant than W-5 V. Our previous studies have reported that the increase of V concentration improves the densification and mechanical properties including structural strength of W-V alloys [9]. The results given in Table 1 also show positive impact of V concentration on W-based materials. That is to say, W-10 V is expected to have the best performance under transient heat loading. But we should note that increasing V



concentration can also significantly reduce the thermal conductivity which is one of the important properties for thermal performance. Under the similar heat loading conditions, the resulting surface temperature of W-10 V is much higher than W-5 V as shown in Fig. 2. This should be the reason for its relatively more severe damage than W-5 V. However, due to its better structural strength, even at higher surface temperatures, the damage of W-10 V is observed to be lower than W-1 V. Thus, W-5 V shows better performance than both lower and higher V containing alloy samples. The results indicate that an appropriate selection of V concentration in W matrix is important to improve the structural stability against high heat loads.

Although some serious cracks on the surface of W-V alloys are observed at higher HHF densities up to 324 MW/m<sup>2</sup>, however no melting/boiling can be seen on surface of these targets. Thus, the melting threshold of these alloys are well above 22.9 MW/(m<sup>2</sup>.s<sup>1/2</sup>), which is considerable good for sintered, low density (< 94%) target samples. From these preliminary results, a considerable improvement in the strength against high heat transient loads of sintered target materials have been achieved by V addition, however we expect that the tolerability of these alloys will be much enhanced by improving the fabrication technique. DBTT is also an important factor to explain the cracking behavior of HHF tested samples, which is strongly depends on testing procedure, production history, precursor power size, composition and microstructures of the sintered materials. Unfortunately the values of DBTT are rarely available in the available literatures for such alloying compositions, as the developed alloys are relatively new for such applications. Further, the size of the present fabricated samples is not large enough to perform such DBTT tests. However, research is in progress to develop high strength fully densified, large size W-V alloys by other sintering techniques and hot rolling as a post-processing is also selected to increase its densification and relevant properties for fusion facing applications. Further investigation including DBTT tests of new improved W-V alloys will be carried out in the future.

## 6. Conclusions

The purpose of this study is to test the newly developed W-V alloys under fusion relevant transient thermal shock, and therefore find better combination of W-V alloy with stable microstructures to resist the surface cracking caused by transient heat loading. Transient high heat load tests by high intensity current pulsed electron beam are performed on three different grades of W-V alloys. The alloys with

lowest V concentration are highly damaged in terms of high crack density. Peak surface temperatures of all samples at all tested HHF densities are well below melting point. An increasing of V concentration gradually improves the structural strength of the alloy targets, while significantly reducing the thermal conductivity. Therefore, with increasing V concentration, W-V alloys have better mechanical strength but undergo much higher surface temperature during heat loading. As a result, the alloy with intermediate V content (5 wt%) shows better cracking resistance against transient heat loads.

## Acknowledgments

This work was supported by the National Magnetic Confinement Fusion Science Program of China under Grant 2013GB109003, the National Nature Science Foundation of China under contract no. 51401012, and the Fundamental Research Funds for the Central Universities under contract no. 50100002015119011. G. H. Lu acknowledges the support from the China National Funds for Distinguished Young Scientists under Grant 51325103, and Kameel Arshad acknowledges the support from Higher Education Commission (HEC) of Pakistan (PD/OS-II/Batch-3).

## References

- [1] M. Roedig, I. Kupriyanov, J. Linke, X. Liu, Z. Wang, J. Nucl. Mat. 417 (2011) 761–764.
- [2] A. Hassanein, T. Sizyuk, I. Konkashbaev, J. Nucl. Mat. 390–391 (2009) 777–780.
- [3] M. Wirtz, J. Linke, G. Pintsuk, G. De Temmerman, G.M. Wright, J. Nucl. Mat. 443 (2013) 497–501.
- [4] J. Linke, Phys. Scr. 2006 (2006) 45.
- [5] G. Federici, P. Andrew, P. Barabaschi, J. Brooks, R. Doerner, A. Geier, A. Herrmann, G. Janeschitz, K. Krieger, A. Kukushkin, A. Loarte, R. Neu, G. Saibene, M. Shimada, G. Strohmayer, M. Sugihara, J. Nucl. Mat. 313–316 (2003) 11–22.
- [6] A. Litnovsky, V.S. Voitsenya, A. Costley, A.J.H. Donn, Nucl. Fusion 47 (2007) 833.
- [7] K. Tobita, S. Nishio, M. Enoda, M. Sato, T. Isono, S. Sakurai, H. Nakamura, S. Sato, S. Suzuki, M. Ando, K. Ezato, T. Hayashi, T. Hirose, T. Inoue, Y. Kawamura, N. Koizumi, Y. Kudo, R. Kurihara, T. Kuroda, M. Matsukawa, K. Mouri, Y. Nakamura, M. Nishi, Y. Nomoto, J. Ohmori, N. Oyama, K. Sakamoto, T. Suzuki, M. Takechi, H. Tanigawa, K. Tsuchiya, D. Tsuru, Fusion Eng. Des. 81 (2006) 1151–1158.
- [8] K. Arshad, W. Guo, J. Wang, M.-Y. Zhao, Y. Yuan, Y. Zhang, B. Wang, Z.-J. Zhou, G.-H. Lu, Int. J. Refract. Metals Hard Mat. 50 (2015) 59–64.
- [9] K. Arshad, M.-Y. Zhao, Y. Yuan, Y. Zhang, Z.-H. Zhao, B. Wang, Z.-J. Zhou, G.-H. Lu, J. Nucl. Mat. 455 (2014) 96–100.
- [10] K. Arshad, M.-Y. Zhao, Y. Yuan, Y. Zhang, Z.-J. Zhou, G.-H. Lu, Mod. Phys. Lett. B 28 (2014) 1450207.
- [11] P. Majerus, R. Duwe, T. Hirai, W. Kühnlein, J. Linke, M. Rödig, Fusion Eng. Des. 75–79 (2005) 365–369.
- [12] J. Linke, T. Loewenhoff, V. Massaut, G. Pintsuk, G. Ritz, M. Rödig, A. Schmidt, C. Thomser, I. Uytendhouwen, V. Vasechko, M. Wirtz, Nucl. Fusion 51 (2011) 073017.
- [13] Y. Zhang, A.V. Ganeev, J.T. Wang, J.Q. Liu, I.V. Alexandrov, Mat. Sci. Eng.: A 503 (2009) 37–40.
- [14] Y. Kitsunai, H. Kurishita, H. Kayano, Y. Hiraoka, T. Igarashi, T. Takida, J. Nucl. Mat. 271–272 (1999) 423–428.